Efficient Multispin Homonuclear Double-Quantum Recoupling for Magic-Angle Spinning NMR: $^{13}C-^{13}C$ Correlation Spectroscopy of U-^{13}C-Erythromycin A

Chad M. Rienstra,[†,‡] Mary E. Hatcher,[‡,§,⊗] Leonard J. Mueller,[‡,▽] Boqin Sun,[‡,∥] Stephen W. Fesik,[⊥] and Robert G. Griffin*[,†,‡]

Department of Chemistry and Center for Magnetic Resonance, Francis Bitter Magnet Laboratory, Massachusetts Institute of Technology, Cambridge, Massachusetts 02139, Department of Chemistry, Brandeis University, Waltham, Massachusetts 02254, and Abbott Laboratories, Abbott Park, Illinois 60064

Received March 25, 1998. Revised Manuscript Received July 13, 1998

Abstract: We introduce a radio frequency (rf) pulse sequence for efficient homonuclear double-quantum dipolar recoupling under magic-angle spinning NMR. The sequence is optimized for two-dimensional double-quantum $^{13}C-^{13}C$ chemical shift correlation spectroscopy in multiple spin systems, such as the U-^{13}C-labeled antibiotic erythromycin A. Spin systems such as this display a wide range of isotropic and anisotropic chemical shifts and, therefore, require a broadband dipolar recoupling sequence that minimizes the errors arising from the interaction of chemical shifts and rf inhomogeneity. The sequence should also preserve the theoretical efficiency over the powder average (∼73%) provided by the C7 experiment of Levitt and co-workers (Lee, Y. K.; Kurur, N. D.; Helmle, M.; Johannessen, O. G.; Nielsen, N. C.; Levitt, M. H. *Chem. Phys. Lett.* **1995**, *242*, 304−309). We satisfy these criteria by combining the standard C7 ($2\pi_\phi-2\pi_{\phi+180}$) elements with π-pulse permuted elements ($\pi_\phi-2\pi_{\phi+180}-\pi_\phi$, in analogy to the MLEV decoupling scheme) to remove error terms over a ±10% range of rf amplitude. The new sequence, which we refer to as CMR7 (*c*ombined *M*LEV *r*efocusing and C*7*), yields for two-spin systems broadband double-quantum filtering efficiencies greater than 70%. For multispin systems, the improved polarization transfer efficiency results in greater cross-peak intensities, facilitating assignment of U-^{13}C-labeled molecules in the solid state.

Introduction

In recent years, solid-state NMR has witnessed a rapid development of techniques aimed at measuring anisotropic interactions in the presence of magic-angle spinning (MAS).[2,3] These techniques provide valuable structural information via site-resolved measurements of interatomic distances[4−6] and the relative orientations of dipole vectors[7−12] and/or chemical shift tensors.[13−17] Such interactions are normally averaged effectively by rapid MAS[18,19] in the context of the CP/MAS experiment,[20,21] which combines cross-polarization[22] and high-power ^1H decoupling[20,23] to provide isotropic chemical shift spectra of high sensitivity and resolution. This spectral dimension provides site resolution but little direct structural information. The latter is usually measured in indirect dimension(s), where radio fre-

† Department of Chemistry, MIT.
‡ Center for Magnetic Resonance, MIT.
§ Brandeis University.
⊥ Abbott Laboratories.
∥ Current address: Magnetic Resonance Department, Schlumberger-Doll Research Laboratory, 110 Schlumberger Dr., Sugarland, TX 77478.
⊗ Current address: Joint Sciences Department, The Claremont Colleges, Claremont, CA 91711.
▽ Current address: Department of Chemistry, University of California at Riverside, Riverside, CA 92521.

(1) Lee, Y. K.; Kurur, N. D.; Helmle, M.; Johannessen, O. G.; Nielsen, N. C.; Levitt, M. H. *Chem. Phys. Lett.* **1995**, *242*, 304−309.
(2) Griffiths, J. M.; Griffin, R. G. *Anal. Chim. Acta* **1993**, *283*, 1081−1101.
(3) Bennett, A. E.; Griffin, R. G.; Vega, S. In *Solid State NMR IV: Methods and Applications of Solid-State NMR*; B. Blumich, Ed.; Springer-Verlag: Berlin, 1994; Vol. 33, pp 1−77.
(4) Thompson, L. K.; McDermott, A. E.; Raap, J.; Vanderwielen, C. M.; Lugtenberg, J.; Herzfeld, J.; Griffin, R. G. *Biochemistry* **1992**, *31*, 7931−7938.
(5) Christensen, A. M.; Schaefer, J. *Biochemistry* **1993**, *32*, 2868−2873.
(6) Lansbury, P. T., Jr.; Costa, P. R.; Griffiths, J. M.; Simon, E. J.; Auger, M.; Halverson, K. J.; Kocisko, D. A.; Hendsch, Z. S.; Ashburn, T. T.; Spencer, R. G. S.; Tidor, B.; Griffin, R. G. *Nat. Struct. Biol.* **1995**, *2*, 990−998.
(7) Feng, X.; Lee, Y. K.; Sandström, D.; Edén, M.; Maisel, H.; Sebald, A.; Levitt, M. H. *Chem. Phys. Lett.* **1996**, *257*, 314−320.
(8) Feng, X.; Verdegem, P. J. E.; Lee, Y. K.; Sandström, D.; Edén, M.; Bovee-Geurts, P.; de Grip, W. J.; Lugtenburg, J.; de Groot, H. J. M.; Levitt, M. H. *J. Am. Chem. Soc.* **1997**, *119*, 6853−6857.
(9) Feng, X.; Eden, M.; Brinkmann, A.; Luthman, H.; Eriksson, L.; Graslund, A.; Antzutkin, O. N.; Levitt, M. H. *J. Am. Chem. Soc.* **1997**, *119*, 12006−12007.
(10) Hong, M.; Gross, J. D.; Griffin, R. G. *J. Phys. Chem. B* **1997**, *101*, 5869−5874.
(11) Hong, M.; Gross, J. D.; Rienstra, C. M.; Griffin, R. G.; Kumashiro, K. K.; Schmidt-Rohr, K. *J. Magn. Reson.* **1997**, *129*, 85−92.
(12) Costa, P. R.; Gross, J. D.; Hong, M.; Griffin, R. G. *Chem. Phys. Lett.* **1997**, *280*, 95.
(13) Levitt, M. H.; Raleigh, D. P.; Creuzet, F.; Griffin, R. G. *J. Chem. Phys.* **1990**, *92*, 6347−6364.
(14) Tycko, R.; Weliky, D. P.; Berger, A. E. *J. Chem. Phys.* **1996**, *105*, 7915−7930.
(15) Weliky, D. P.; Tycko, R. *J. Am. Chem. Soc.* **1996**, *118*, 8487−8488.
(16) Schmidt-Rohr, K. *J. Am. Chem. Soc.* **1996**, *118*, 7601−7603.
(17) Bennett, A. E.; Weliky, D. P.; Tycko, R. *J. Am. Chem. Soc.* **1998**, *120*, 4897−4898.
(18) Andrew, E. R.; Bradbury, A.; Eades, R. G. *Nature (London)* **1958**, *182*, 1659.
(19) Lowe, I. J. *Phys. Rev. Lett.* **1959**, *2*, 285.
(20) Schaefer, J.; Stejskal, E. O. *J. Am. Chem. Soc.* **1976**, *98*, 1031.
(21) Maricq, M. M.; Waugh, J. S. *J. Chem. Phys.* **1979**, *70*, 3300.
(22) Pines, A.; Gibby, M. G.; Waugh, J. S. *J. Chem. Phys.* **1973**, *59*, 569−590.
(23) Bennett, A. E.; Rienstra, C. M.; Auger, M.; Lakshmi, K. V.; Griffin, R. G. *J. Chem. Phys.* **1995**, *103*, 6951.

10.1021/ja9810181 CCC: $15.00
Published on Web 10/06/1998

quency (rf) perturbations are applied to recover NMR observables that are correlated with structural parameters.

The behavior of the spin system under rf modulations that interfere with MAS-assisted averaging is customarily described by coherent averaging theory.[24,25] In principle, any term in the Hamiltonian with unique spin and/or spatial symmetry can be measured independently of other terms. However, accomplishing this in a manner that is efficient and free of contamination is a continuing challenge, particularly for the class of experiments that recover homonuclear dipole−dipole couplings. For example, the first rf-driven homonuclear recoupling experiments, such as DRAMA[26,27] and RFDR,[28,29] were designed solely with rotor-synchronized $\pi/2$ and π pulses. Even in the ideal pulse limit, these sequences depend on chemical shifts, both isotropic and anisotropic, to the detriment of dipolar recoupling efficiency. The spin dynamics responsible for this compromised efficiency may be understood with the fictitious spin $^1/_2$ theory,[30,31] where, in the appropriate dipolar subspace,[32] the residual chemical shifts are orthogonal to the recovered dipolar interaction. The exact dipolar evolution is described by spin decoupling theory, whereby large residual chemical shifts quench the dipolar interactions.[33]

The dependence on chemical shifts is, to some extent, inherent in the laboratory frame spin dynamics, and several sequences have been proposed to avoid this shortcoming by using a continuous (windowless) rf irradiation field that is large compared to the chemical shifts. Under these conditions, chemical shift spin terms are, to first approximation, averaged to zero. This approach was first applied to dipolar recoupling with the MELODRAMA sequence,[34] which generates a pure double-quantum (DQ) dipolar Hamiltonian without interference from chemical shifts terms. Similarly, the DRAWS sequence[35−37] effectively averages chemical shifts, albeit at the cost of introducing a zero-quantum (ZQ) component, which is undesirable for some applications.

An additional theoretical consideration for sequences of this type, demonstrated by Levitt and co-workers,[1,38] shows that individual spatial components can be selected so that recoupling occurs independent of rotor phase (specifically the azimuthal angle, γ_{PR}, relating the principal axis frame of the dipolar interaction to the rotor-fixed frame). Over the powder average, elimination of the rotor-phase dependence increases the theoretical double-quantum filtration (DQF) efficiency from ∼52% (with MELODRAMA[34] or DRAWS[35]) to ∼73% (with HORROR[38] or C7[1]). This increased efficiency is particularly useful for applications such as correlation spectroscopy and DQF of strongly coupled spin pairs, where the sensitivity of the experiment depends on the mixing efficiency.

However, the often unavoidable presence of rf errors, especially inhomogeneity, complicates this picture. Although some recent probe designs[39] based on loop-gap resonators[40] can provide extremely high rf homogeneity over the full sample volume (<1−2% full width at half-maximum (fwhm) in the nutation[41] dimension), most solid-state NMR probes use solenoid coil geometries that have distributions of rf field amplitude of 5−10% over the sample volume. In addition, amplifier and/or probe instabilities can contribute to short- or long-term fluctuations in rf amplitude. Therefore, in the development of recoupling sequences, it is necessary to consider explicitly the effects that rf inhomogeneity has upon the recoupling dynamics; these effects are usually not explained fully by basic theoretical treatments.

For example, it has been observed experimentally that the C7 sequence works most effectively when the rf carrier is centered between the two signals of interest,[8] where the chemical shift in the DQ subspace[30,31] vanishes. When this condition is not satisfied, a residual offset appears as a cross-term between the rf inhomogeneity and chemical shift (described below), producing an effective quenching field orthogonal to the recoupled interaction. This results in spin dynamics analogous to rotational resonance[13,42,43] and frequency-selective heteronuclear dipolar recoupling (FDR[44,45]). In such selective sequences, the quenching field may be exploited to eliminate the effects of strong couplings in order to measure weaker interactions in a multispin system.[43−48] However, when the goal is to recouple many spins with high efficiency for correlation spectroscopy or DQF, it is desirable to eliminate the effects of chemical shift offset entirely. This goal has motivated the development of an improved version of the MELODRAMA sequence which uses phase-compensated π pulses superimposed upon the basic sequence to provide correction for rf errors.[49] The result is comparable to the DRAWS sequence,[35−37] with the additional advantage of maintaining a pure DQ Hamiltonian.

Despite the experimental reliability of these two sequences, each promises only ∼52% maximum theoretical DQF efficiency. Clearly, development of a robust compensation scheme, similar to that for MELODRAMA or DRAWS, would be highly useful for the more efficient C7 sequence. Yet, to retain this efficiency advantage, the solution must not introduce rotor-phase dependence or otherwise disrupt the sequence symmetry. In the following sections, we will demonstrate theoretically how rf field inhomogeneity directly affects the averaging of chemical shift terms in the C7 sequence and propose a method for

(24) Haeberlen, U.; Waugh, J. S. *Phys. Rev.* **1968**, *175*, 453.
(25) Haeberlen, U. *High-Resolution NMR in Solids: Selective Averaging*; Academic Press: New York, 1976.
(26) Tycko, R.; Dabbagh, G. *Chem. Phys. Lett.* **1990**, *173*, 461−465.
(27) Tycko, R.; Smith, S. O. *J. Chem. Phys.* **1993**, *98*, 932−943.
(28) Bennett, A. E.; Ok, J. H.; Griffin, R. G.; Vega, S. *J. Chem. Phys.* **1992**, *96*, 8624−8627.
(29) Bennett, A. E.; Rienstra, C. M.; Griffiths, J. M.; Zhen, W.; Lansbury, P. T., Jr.; Griffin, R. G. *J. Chem. Phys.* **1998**, *108*, 9463−9479.
(30) Wokaun, A.; Ernst, R. R. *J. Chem. Phys.* **1977**, *67*, 1752.
(31) Vega, S. *J. Chem. Phys.* **1978**, *68*, 5518.
(32) Munowitz, M. *Coherence and NMR*; Wiley: New York, 1988.
(33) Waugh, J. S. *J. Magn. Reson.* **1982**, *50*, 30.
(34) Sun, B.-Q.; Costa, P. R.; Kocisko, D. A.; Lansbury, P. T., Jr.; Griffin, R. G. *J. Chem. Phys.* **1995**, *102*, 702−707.
(35) Gregory, D. M.; Mitchell, D. J.; Stringer, J. A.; Kiihne, S.; Shiels, J. C.; Callahan, J.; Mehta, M. A.; Drobny, G. P. *Chem. Phys. Lett.* **1995**, *246*, 654.
(36) Mehta, M. A.; Gregory, D. M.; Kiihne, S.; Mitchell, D. J.; Hatcher, M. E.; Shiels, J. C.; Drobny, G. P. *Solid State Nucl. Magn. Reson.* **1996**, *7*, 211−288.
(37) Gregory, D. M.; Mehta, M. A.; Shiels, J. C.; Drobny, G. P. *J. Chem. Phys.* **1997**, *107*, 28−42.
(38) Nielsen, N. C.; Bildsøe, H.; Jakobsen, H. J.; Levitt, M. H. *J. Chem. Phys.* **1994**, *101*, 1805−1812.
(39) Larsen, F. H.; Daugaard, P.; Jakobsen, H. J.; Nielsen, N. C. *J. Magn. Reson. A* **1995**, *115*, 283−286.
(40) Froncisz, W.; Hyde, J. S. *J. Magn. Reson.* **1982**, *47*, 515−521.
(41) Bax, A. *Two-Dimensional Nuclear Magnetic Resonance in Liquids*; Delft University Press: Dordrecht, Holland, 1980.
(42) Raleigh, D. P.; Levitt, M. H.; Griffin, R. G. *Chem. Phys. Lett.* **1988**, *146*, 71−76.
(43) Costa, P. R.; Sun, B. Q.; Griffin, R. G. *J. Am. Chem. Soc.* **1997**, *119*, 10821−10830.
(44) Bennett, A. E.; Becerra, L. R.; Griffin, R. G. *J. Chem. Phys.* **1994**, *100*, 812−814.
(45) Bennett, A. E.; Rienstra, C. M.; Lansbury, P. T., Jr.; Griffin, R. G. *J. Chem. Phys.* **1996**, *105*, 10289−10299.
(46) Costa, P. R. Ph.D. Thesis, Massachusetts Institute of Technology, 1996.
(47) Costa, P. R.; Sun, B.-Q.; Griffin, R. G. Manuscript in preparation.
(48) Munowitz, M. *Mol. Phys.* **1990**, *71*, 959−978.
(49) Rienstra, C. M.; Sun, B.-Q.; Hu, J. G.; Costa, P. R.; Hatcher, M. E.; Herzfeld, J.; Griffin, R. G. Manuscript in preparation.

minimizing the residual shifts on a short time scale. The compensation scheme slightly restricts the sampling interval but effectively scales the cross-terms between rf errors and chemical shift offsets to provide broadband performance under typical experimental conditions. Because the compensation involves implementation of MLEV-type composite rotations and supercycles[50] to refocus error terms, we refer to the new sequence as *c*ombined *M*LEV *r*efocusing and C*7* (CMR7). The utility of this broadband sequence is demonstrated in a 2D correlation spectrum of the U-^{13}C-labeled antibiotic erythromycin A.

Experimental Methods

NMR Experiments. NMR spectra were acquired on custom-designed spectrometers operating at ^{1}H frequencies of 397.8 (9.4 T), 317.4 (7.4 T), or 198.3 MHz (4.7 T) with custom-designed triple- or quadruple-resonance MAS probes implementing transmission line isolation and tuning circuits.[51−53] At the high frequency, standing wave losses are minimized by periodically altering the characteristic impedance along the main transmission line. This approach allows the final tuning and matching to be removed from the magnet bore, leaving space for high-voltage fixed capacitors (American Technical Ceramics, Huntington Station, NY) and high-voltage variable capacitors (Polyflon Co., Norwalk, CT, or Jennings Technology Co., San Jose, CA), while maintaining optimal overall circuit efficiency. Solenoid sample coils wrapped from Teflon-coated wire were mounted in spinner modules (4 mm for the 397.8- and 317.4-MHz probes, 5 mm for the 198.3-MHz probe) from Chemagnetics/Otsuka Electronics USA (Fort Collins, CO). Unless indicated otherwise, rotors were packed with enough sample to fill the entire usable volume as specified by the manufacturer. This resulted in rf inhomogeneity of 5−10% fwhm. Recycle delays were 2−4 s.

All experiments employed some version of the pulse sequences presented in Figure 1. Ramped CP[54] from ^{1}H to ^{13}C created the initial transverse polarization. In the two-dimensional (2D) version of the sequence, a period of evolution under TPPM decoupling[23] is used to encode chemical shifts in the indirect dimension. In the one-dimensional (1D) experiment, transverse magnetization is immediately stored longitudinally with a $\pi/2$ pulse. In either case, mixing is performed according to the phase modulation scheme presented in Figure 1, where compensation for residual rf errors is accomplished by alternation of C_p and C_p' subcycles. The basic C_p elements are combined to provide a complete CMR7 cycle over four rotor periods. Improved long-time behavior (not discussed in detail here) is obtained by expanding the basic unit with phase inversions and cyclic permutations to create the supercycle as indicated in Figure 1. For the 2D experiment, the total mixing time was chosen to be a multiple of $4\tau_r$, so that residual errors between the CSA and rf inhomogeneity would be refocused most effectively. Spectral intensities in all cases are computed by integration of the line shape and include correction for natural abundance background.

Phase cycles for the DQF experiments followed standard procedures for selection of DQ coherence,[55] in addition to spin temperature alternation of the ^{1}H reservoir. The 2D chemical shift correlation experiment incorporated phase cycles for pure phase detection in both dimensions developed by Ruben and co-workers.[56]

^{13}C-Labeled Samples. All U-^{13}C,^{15}N-labeled amino acids (Cambridge Isotope Laboratories, Andover, MA) were, where indicated, diluted in natural abundance material and recrystallized by slow evaporation from aqueous solution. U-^{13}C-Oxalic acid (also from CIL) was dissolved with 1 equiv of NH_4OH in aqueous solution and recrystallized by slow evaporation.

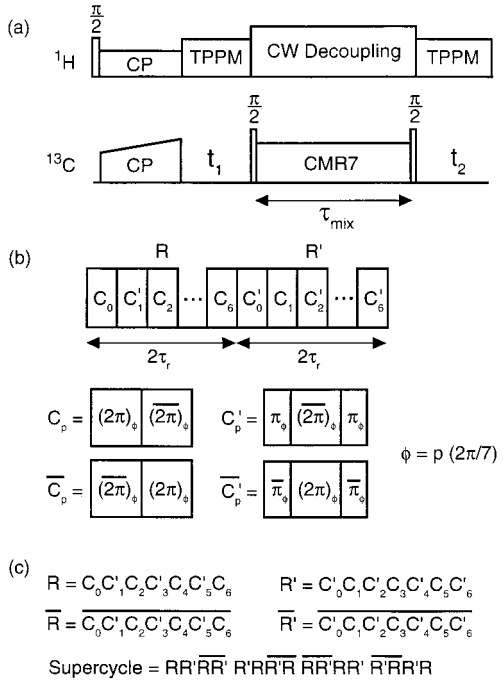

Figure 1. CMR7 rf pulse sequence. (a) General sequence for double-quantum dipolar recoupling in the framework of CP-MAS spectroscopy. Following ramp CP and an optional period of chemical shift evolution, sum polarization is stored longitudinally and the mixing sequence initiated. After mixing, observable coherence is read out with a $\pi/2$ pulse. During the evolution and acquisition periods, TPPM ^{1}H decoupling[23] is implemented; during the mixing period, high-power resonant CW decoupling is used. (b) Basic CMR7 mixing sequence, constructed from C_p units of various symmetry. Notation is consistent with that of Lee et al.[1] The complete sequence is composed in a manner that most rapidly refocuses large, isotropic error terms. (c) Full supercycling of the compensation scheme for achieving quantitative long-time results. Phase inversions and cyclic permutations of the basic CMR7 sequence help to maximize coherence of the appropriate order. References to C7 and CMR7 indicate the $N = 2$, $n = 7$ sequence unless explicitly stated otherwise.

U-^{13}C-Erythromycin A was prepared by fermentation of *Saccharopolyspora erythraea* strain ER598 in a salt medium containing 1% D-glucose-U-$^{13}C_6$ as the sole source of carbon. Two liters of the medium was dispensed at 50 mL in 500-mL Erlenmeyer flasks. Vegetative inoculum grown in a rich organic medium was washed and used at 1%. The flasks were incubated at 32 °C on a rotary shaker operating at 225 rpm for 6 days. U-^{13}C-Erythromycin was purified from 1500 mL of beer from two separate shake flask experiments by extracting twice with equal volumes of CH_2Cl_2 at pH 9. The extracts were pooled, dried, and digested into 2.5 mL of a solvent system consisting of *n*-hexane/ethyl acetate/aqueous potassium phosphate (0.02 M, pH 7) (3:7:5). The mixture was subject to countercurrent chromatography in an Ito multilayer Planet Coil centrifuge, with the upper phase mobile. Fractions were monitored on the basis of bioactivity against *Streptomyces aureus* and from ^{1}H NMR spectra. U-^{13}C-Erythromycin was crystallized using ethyl acetate and *n*-hexane to yield 39 mg with >98% labeling efficiency based on an analysis of the C-1′ resonance. These conditions produced the dehydrated form for solid-state NMR studies.[81,82]

Background

Homonuclear recoupling sequences are readily described within the formalism of average Hamiltonian theory (AHT).[24,25] For simplicity, we assume that the abundant ^{1}H spins are removed from the dynamics completely by high-power decou-

(50) Levitt, M. H.; Freeman, R.; Frenkiel, T. *J. Magn. Reson.* **1982**, *50*, 157−160.
(51) Holl, S. M.; McKay, R. A.; Gullion, T.; Schaefer, J. *J. Magn. Reson.* **1990**, *89*, 620−626.
(52) McKay, R. A. United States Patent 4,446,431, 1984.
(53) McKay, R. A. Private communication, 1995.
(54) Wu, X.; Zilm, K. W. *J. Magn. Reson. A* **1993**, *104*, 154−165.
(55) Wokaun, A.; Ernst, R. R. *Chem. Phys. Lett.* **1977**, *52*, 407.
(56) States, D. J.; Haberkorn, R. A.; Ruben, D. J. *J. Magn. Reson.* **1982**, *48*, 286.

pling. (This assumption is not always justified, but we will demonstrate that such a limit can be achieved experimentally in the spinning speed regimes used here.) The rotating-frame Hamiltonian, therefore, consists of terms corresponding to the low-γ spin chemical shifts, dipole−dipole couplings, and an applied rf field:[57]

$$H = H_{int} + H_{rf} \tag{1a}$$

$$H_{int} = \omega_j(t)S_{jz} + \omega_k(t)S_{kz} + \omega_{D_{jk}}(t)(3S_{jz}S_{kz} - \boldsymbol{S}_j\cdot\boldsymbol{S}_k) \tag{1b}$$

$$H_{rf} = \omega_1(t)[(S_{jx} + S_{kx})\cos\varphi(t) + (S_{jy} + S_{ky})\sin\varphi(t)] \tag{1c}$$

where the time dependence of the coefficients of (1b) are expressed as

$$\omega_j(t) = \sum_{m=-2}^{2} \omega_0\delta_j^{(m)}\, e^{im\omega_r t} \tag{2}$$

and

$$\omega_{D_{jk}}(t) = \sum_{m=-2}^{2} \omega_{D_{jk}}^{(m)}\, e^{im\omega_r t} \tag{3}$$

Complete expressions for the chemical shift anisotropy $\omega_0\delta_j^m$ may be found in ref 13, although the coefficients are not important in the following, where averaging is designed to eliminate their effects. The time-dependent forms for the dipole−dipole coupling, however, will be used further and, therefore, are defined (assuming MAS[18,19]) as

$$\omega_{D_{jk}}^{(0)} = 0 \tag{4a}$$

$$\omega_{D_{jk}}^{(\pm1)} = -\frac{\omega_{D_{jk}}}{2\sqrt{2}}\sin(2\beta_{PR})\, e^{\pm i\gamma_{PR}} \tag{4b}$$

$$\omega_{D_{jk}}^{(\pm2)} = \frac{\omega_{D_{jk}}}{4}\sin^2(\beta_{PR})\, e^{\pm 2i\gamma_{PR}} \tag{4c}$$

where the angles β_{PR} and γ_{PR} describe the transformation from the principal axis system of the dipole vector to the rotor-fixed coordinate system.[58] The dipolar coupling constant in angular units is

$$\omega_{D_{jk}} = -\frac{\mu_0}{4\pi}\frac{\gamma_j\gamma_k\hbar}{r_{jk}^3} \tag{5}$$

When the time dependence of H_{rf} involves nonorthogonal rf phases, the Cartesian basis may be cumbersome for purposes of calculating the interaction frame Hamiltonian. Therefore, in the following, we use irreducible spherical tensor operators in the convention of Spiess.[58] This notation permits both the spatial and spin parts of the Hamiltonian to be expressed in similar forms and, in particular, simplifies the calculation of spin terms that arise upon general (i.e., nonorthogonal) phase shifts of the rf irradiation. Thus, the phases of all terms of the Hamiltonian may be described together in a convenient form. In this basis, single-spin operators are expressed as

$$T_{10}^j = S_{jz} \tag{6a}$$

and the two-spin operators as

$$T_{20}^{jk} = \frac{1}{\sqrt{6}}(3S_{jz}S_{kz} - \boldsymbol{S}_j\cdot\boldsymbol{S}_k) \tag{6b}$$

$$T_{2\pm2}^{jk} = \frac{1}{2}S_j^{\pm}S_k^{\pm} \tag{6c}$$

Substituting these terms into eq 1 and following the treatment of Lee et al.,[1] we examine the Hamiltonian in the interaction frame of the rf field,

$$\tilde{H}(t) = U_{rf}H_{int}U^{-1}{}_{rf} = \sum_Q\sum_{\lambda\mu lm}\tilde{\omega}_{\lambda\mu lm}^Q(t - t_p^0)\times \exp[i2\pi(Nm - \mu)p/n]T_{\lambda\mu}^Q \tag{7}$$

defined over the time of the pth subcycle, $t_p^0 \le t < t_{p+1}^0$. The variable Q refers to the type of interaction, l the rank with respect to spatial modulation, m the spatial rotational component ($m = \{-l,-l+1, ..., l\}$), λ the rank with respect to spin modulations, and μ the spin rotational component ($\mu = \{-\lambda,-\lambda+1, ..., \lambda\}$).

The values of the coefficients

$$\tilde{\omega}_{\lambda\mu lm}^Q(\tau) = i^\mu d_{\mu0}^\lambda(\beta_{rf}(\tau))\tilde{\omega}_{\lambda0lm}^Q \exp[im\omega_r(\tau + t^0)] \tag{8}$$

are given in general by the reduced Wigner functions $d_{\mu0}^\lambda$ [59] and the overall spin rotation angle β_{rf}, which is a function of time, dependent on the sequence being investigated.

For the Cn class of experiments, where n phase-shifted elements are implemented over N rotor periods (e.g., for C7, $n = 7$ and $N = 2$), the rf field is chosen to match an appropriate multiple of the spinning speed, as defined by

$$\omega_1 = \frac{2n}{N}\omega_r \tag{9}$$

However, in practice this match is only approximately true across the entire sample volume due to rf inhomogeneity, and some effort must be made to understand the effects of deviation from the ideal value. One approach to analyzing the effect of an inhomogeneous rf field is to partition H_{rf} into a large term, $|\omega_1(t)|$, which defines the interaction frame, and a smaller rf inhomogeneity term, $|\Delta\omega_1(t)|$, included in H_{int}. Analysis of the effective Hamiltonian

$$\bar{\tilde{H}} = \bar{\tilde{H}}^{(0)} + \bar{\tilde{H}}^{(1)} + \bar{\tilde{H}}^{(2)} + \cdots \tag{10}$$

through second order, defined as

$$\bar{\tilde{H}}^{(0)} = \frac{1}{\tau_c}\int_0^{\tau_c}\tilde{H}(t)\,dt \tag{11a}$$

$$\bar{\tilde{H}}^{(1)} = \frac{-i}{2\tau_c}\int_0^{\tau_c}dt_2\int_0^{t_2}[\tilde{H}(t_1),\tilde{H}(t_2)]\,dt_1 \tag{11b}$$

$$\bar{\tilde{H}}^{(2)} = \frac{-1}{6\tau_c}\int_0^{\tau_c}dt_1\int_0^{t_1}dt_2\int_0^{t_2}dt_3([\tilde{H}(t_1),[\tilde{H}(t_2),\tilde{H}(t_3)]] + [\tilde{H}(t_3),[\tilde{H}(t_2),\tilde{H}(t_1)]]) \tag{11c}$$

results in error terms which arise in $\bar{\tilde{H}}^{(1)}$ and $\bar{\tilde{H}}^{(2)}$, involving $|\Delta\omega_1(t)|$ and $(\omega_j + \omega_k)$. This is a general approach to calculating

(57) Mehring, M. *Principles of High-Resolution NMR in Solids*; Springer-Verlag: Berlin, 1983.

(58) Spiess, H. W. In *NMR Basic Principles and Progress*; Diehl, P., Fluck, E., Kosfeld, E., Eds.; Springer: Berlin, 1978; Vol. 15, pp 58−214.

(59) Sakurai, J. J. *Modern Quantum Mechanics*; Cummings Publishing: Menlo Park, CA, 1985.

Table 1. Coefficients from AHT Calculation ($\tilde{\ };\bar{\ }H^{(0)}$) for the General Windowless Recoupling Scheme Defined in Figure 1[a]

$\lambda\mu l$	k	a	a'	b	b'
102	1	$Nmn\sin\left(\frac{Nm\pi}{n}\right)$	$Nmn\sin\left(\frac{Nm\pi}{n}\right)$	$-2n^2 s\sin(2\pi s)$	$-4n^2 s\sin(\pi s)\cos\left(\frac{Nm\pi}{2n}\right)$
222	$\sqrt{\frac{3}{2}}\frac{n^2 s}{Nm}$	$-4ns\sin\left(\frac{Nm\pi}{n}\right)$	$-4ns\sin\left(\frac{Nm\pi}{n}\right)$	$Nm\sin(4\pi s)$	$2Nm\sin(2\pi s)\cos\left(\frac{Nm\pi}{2n}\right)$

[a] The effect of rf inhomogeneity is explicitly included in the variable s, which expresses deviation from the ideal value ($s = 1$). The coefficients a and b refer to the C_p subcycles, a' and b' to the C'_p subcycles. Note that all functions of the form $k(a + b)$ are even with respect to the s, so phase inversion alone does not remove the residual error. Through this level of AHT, all other spin components vanish according to eq 15.

the relative magnitude of various higher-order contributions to the total effective Hamiltonian and has been used to derive another compensated C7 sequence.[60]

In the present context, we are primarily concerned with the effect of rf inhomogeneity on the spin terms, so we choose an alternative form of analysis that is well suited for excitations with symmetry such as the elements from which CMR7 is composed. Because each subcycle (C_p or C'_p) consists of rotations with phases ϕ and $\phi + \pi$, constructed as in Figure 1b, the sequence is periodic over the element ($U_{rf} = 1$), independent of the exact rf amplitude. This allows the average spin terms to be conveniently incorporated into $\bar{\tilde{H}}^{(0)}$ without making any assumptions about the relative magnitude of the rf inhomogeneity by including explicit dependence on a rf field scaling factor,

$$s = \omega_{1,actual}/\omega_{1,ideal} \tag{12}$$

We proceed with direct calculation of the coefficients and find, after algebraic simplification, that each term has the general form

$$\bar{\omega}^Q_{\lambda\mu lm} = \Phi(p)c^Q\, k_{\lambda\mu l}(a_{\lambda\mu lm} + b_{\lambda\mu lm}) \tag{13}$$

where the first factor

$$\Phi(p) = \exp[i2\pi(Nm - \mu)p/n] \tag{14}$$

is a phase depending on several variables. Incrementing p from one subcycle to the next provides a means for selecting desired spin (μ) and spatial (m) components by choice of the pulse sequence parameters N and n. Upon summation of the phases over the complete cycle, we find the function

$$\sum_{p=0}^{n-1}\frac{\Phi(p)}{n} = \begin{cases} 1 & Nm - \mu = n(\text{integer}) \\ 0 & Nm - \mu \neq n(\text{integer}) \end{cases} \tag{15}$$

The second factor of eq 13 does not explicitly depend on the spin component (μ):

$$c^{jk} = c_0\omega^{(m)}_{D_{jk}} \tag{16a}$$

$$c^{j} = c_0\delta^{(m)}_j\omega_0 \tag{16b}$$

$$c^{jk} = \left[\frac{\exp[iNm\pi/n]}{\pi(Nm - 2\lambda ns)(Nm + 2\lambda ns)}\right] \tag{16c}$$

The expressions for the spin components $k_{\lambda\mu l}(a_{\lambda\mu lm} + b_{\lambda\mu lm})$, gathered in Table 1, contain the explicit dependence upon rf inhomogeneity as a function of s. The most important result is the significant error term that arises when $s \neq 1$ and the isotropic chemical shift (in the DQ subspace, $\omega^j_{1020} + \omega^k_{1020}$) is nonzero. With the C_p element alone, the longitudinal term has a strong dependence on s, as illustrated in Figure 2. The z-component can be inverted over the next element (C'_{p+1}) by cyclic permutation of a π rotation.[50,61] Combination of these two elements cancels the (large) isotropic error term (through $O(s - 1)^2$) over the time scale of $^4/_7\tau_r$. The isotropic error term would not be averaged by the standard C7 phase-shifting alone (through the symmetry of eq 15) because the error term phase is invariant with respect to the shifts in rf phase (i.e., for $m = \mu = 0$, $\Phi(p) = 1$). Additional, smaller error terms due to the interaction of CSA with the inhomogeneity are averaged on a time scale of $4\tau_r$.

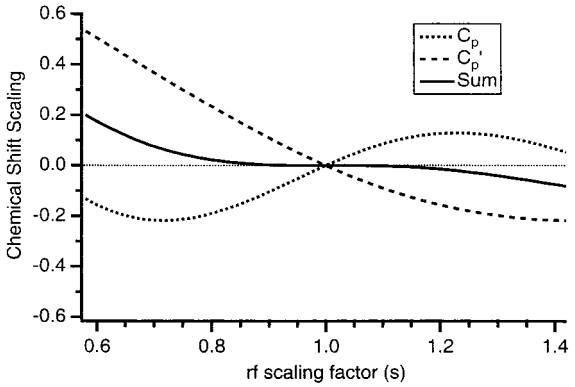

Figure 2. Residual isotropic chemical shift due to rf inhomogeneity for the basic subcycle $C_p = 2\pi_\varphi 2\pi_{\varphi+180}$ and the cyclic permutation $C'_p = \pi_\varphi 2\pi_{\varphi+180}\pi_\varphi$. See Table 1 for analytic forms. Combination of the two in the manner shown in Figure 1 refocuses isotropic chemical shift error terms (to this level of approximation) over a time scale of $^4/_7\tau_r$, and anisotropic terms over $4\tau_r = 2\tau_c$.

The analytic forms of Table 1 provide a simple method for calculating the magnitude of recoupled interactions in a general manner. The expression for $\omega_{2\pm22\pm1}$(with $s = 1$, i.e., ideal rf irradiation) can be evaluated over the general Cn cycle as

$$\sum_{p=0}^{n-1}\frac{\bar{\omega}_{2\pm22\pm1}}{n} = \frac{i3\sqrt{2}}{2\pi}\frac{n^3(\exp[iN2\pi/n] - 1)}{N(N^2 - 16n^2)}\omega^{jk}_D\sin 2\beta_{PR} \tag{17}$$

This expression allows convenient evaluation of the scaling factors for alternative formulations of the Cn sequences. For example, for $N = 2$ and $n > 6$, only a single spatial component is selected for each spin component ($m = \pm1$ for $\mu = \pm2$). The exact scaling factor depends on the value of n; for $n = 7$, the familiar C7 scaling factor is recovered:

$$|\bar{\omega}_{2\pm22\pm1}| = |-\frac{343(i + e^{i\pi/14})}{520\pi\sqrt{2}}| \cong 0.232\omega^{jk}_D\sin 2\beta_{PR} \tag{18}$$

In the limit where $n \rightarrow \infty$, the dipolar scaling factor under

(60) Hohwy, M.; Jakobsen, H. J.; Edén, M.; Levitt, M. H.; Nielsen, N. C. *J. Chem. Phys.* **1998**, *108*, 2686−94.

(61) Waugh, J. S. *J. Magn. Reson.* **1982**, *49*, 517−21.

double-quantum dipolar recoupling is

$$|\bar{\omega}_{2\pm22\pm1}| = \frac{3}{8\sqrt{2}} \cong 0.265\omega_D^{jk} \sin 2\beta_{PR} \qquad (19)$$

Therefore, when it is experimentally feasible, more rapid phase shifting (and correspondingly higher rf amplitudes) may be used to increase the scale factor by up to ~14% within this limit. This may be useful for the measurement of weak couplings in some circumstances.

Of more general use for correlation spectroscopy are the cases where $n = 7$ and $N = 5$ or 9. These solutions satisfy the symmetry constraints in a manner similar to that of the $N = 2$ case; i.e., only DQ spin terms ($\mu = \pm 2$) with a single spatial component ($m = \mp 1$ for $N = 5$, $m = \pm 1$ for $N = 9$) remain over the cycle. With respect to the sample rotation, the rf phases are shifted less rapidly as N increases, and the intuitive expectation of a less favorable dipolar scaling factor results:

$$|\bar{\omega}_{2\pm22-1}| = |\frac{343(i + e^{i\pi/14})}{1265\pi\sqrt{2}}| \cong 0.095\omega_D^{jk} \sin 2\beta_{PR} \quad \text{for } N = 5 \quad (20a)$$

$$|\bar{\omega}_{2\pm22\pm1}| = |-\frac{343(i + e^{i\pi/14})}{2109\pi\sqrt{2}}| \cong 0.057\omega_D^{jk} \sin 2\beta_{PR} \quad \text{for } N = 9 \quad (20b)$$

However, the reduction in scaling factor may be an acceptable compromise for applications at high MAS rates because the required rf field amplitude is decreased approximately by the same percentage as the dipolar scaling factor. In the MAS regime of 10−20 kHz and beyond, achieving $\omega_1 = (2n/N)\omega_r$ may not be experimentally feasible for $N = 2$. In these cases, the sequences with $N = 5$ or 9 would allow more reasonable rf field amplitudes to be used. For $^{13}C-^{13}C$ chemical shift correlation spectroscopy in U-^{13}C-labeled samples, the higher N alternatives imply increasing the optimal mixing time for one-bond transfer from ~1 to 2.5 and 4 ms (for $N = 5$ and 9, respectively). Provided that appropriate ^1H decoupling conditions are maintained (see below), the additional mixing time is not expected to cause significant signal loss, allowing the full advantage of the C7 line shape to be exploited at higher MAS rates. As discussed in more detail below, with the $N = 2$ CMR7 sequence, ~1 ms mixing provides strong one-bond correlations and many two-bond correlations in all U-^{13}C-labeled systems studied thus far. Similar behavior would be expected for the higher N alternatives with proportionately longer mixing times. Here we also note that the form for the ω_{222m} component in Table 1 indicates a scaling of the dipolar coupling that depends explicitly on the rf amplitude. The implications of this effect with respect to quantitative distance measurements with CMR7 will be discussed in a forthcoming publication.[62]

For the MELODRAMA[34] pulse sequence (where $n = 4$, $N = 2$) although the overall symmetry of the sequence does not cause terms such as $\mu = 0$, $m = \pm 2$ to vanish, the symmetry described in Lee et al.[1] (eq 15) is a sufficient but not necessary condition for removal of all CSA terms. Direct examination of the terms a_{102m} and b_{102m} in Table 1 shows that the subcycle averaging of all chemical shift terms in the MELODRAMA sequence is accomplished on half-rotor period time scale, rather than the two-rotor period time scale of the full C7 averaging. For $\mu = 0$, this is identically true, as the term a_{102m} vanishes when $Nm = n$(integer). The residual chemical shift interactions (b_{102m}) (for $s \neq 1$) can be minimized by improved compensation schemes.[49] The remaining shortcoming of the MELODRAMA sequence is that both $m = 1$ and $m = -1$ spatial components are recoupled, leading to a sin γ_{PR} dependence in the average recoupled interaction. Integration over γ_{PR} then reduces the maximum double-quantum filtering efficiency from ~73% to ~52%. (For C7/CMR7, the phase, but not the magnitude, of the recoupled interaction depends on γ_{PR}.)

(62) Rienstra, C. M.; Mueller, L. J.; Hatcher, M. E.; Griffin, R. G. Manuscript in preparation.

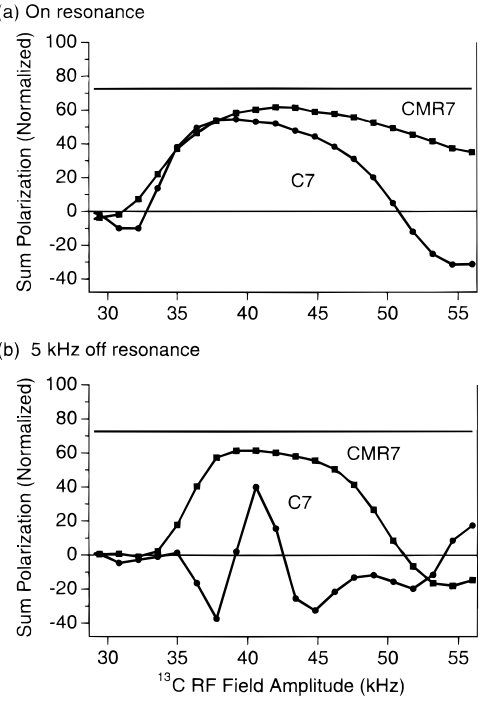

Figure 3. Experimental ^{13}C double-quantum filtration (DQF) efficiencies in U-^{13}C,^{15}N-glycine. Experiments were performed at 397.8-MHz ^1H frequency and 5.95-kHz (±5 Hz) MAS rate, with 670-μs double-quantum excitation ($\tau_{mix} = 1.34$ ms) under 125-kHz resonant CW ^1H decoupling. Decoupling power was reduced to 80-kHz TPPM (5.8 μs, ±7.5°) during acquisition. The sample (~10 mg) was packed in the middle ~20% of the 4-mm rotor (Chemagnetics/Otsuka Electronics) sample volume to ensure optimal rf homogeneity. (Steady-state rf field amplitudes and homogeneity (2−3% fwhm) were determined with standard nutation experiments.[41]) The solid horizontal line indicates the maximum theoretical C7/CMR7 DQF efficiency. (a) Carrier frequency centered between the two peaks of interest. (b) Carrier frequency offset by 5 kHz from center.

Results and Discussion

Radio Frequency Error Compensation and $^1H-^{13}C$ Decoupling Dynamics. Figure 3 illustrates the dependence of C7 and CMR7 DQF efficiency on rf amplitude for two different carrier offsets. The total mixing time, consisting of one-half double-quantum excitation and one-half reconversion, is chosen to maximize the theoretical DQF efficiency (~73%). For a 2-kHz dipolar coupling, this maximum occurs at ~1.3 ms, which, in this case, is approximately equal to $4\tau_c$ ($8\tau_r$). The even integer multiple of the pulse sequence cycle is used to ensure that all anisotropic chemical shifts are averaged as completely as possible. Sampling within the cycle yields small oscillations due to the combination of CSA and rf error.

The results presented in Figure 3 were obtained under circumstances that are optimized beyond what is typical forstandard solenoid sample coils. Only the center portion of the available sample volume was used, yielding a small rf field

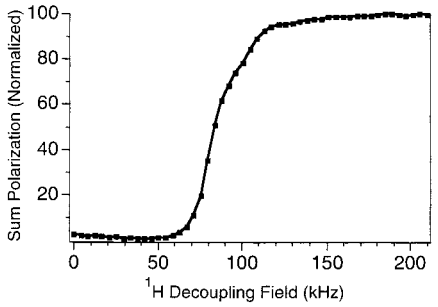

Figure 4. Dependence of DQF efficiency on ^{1}H CW decoupling field strength during mixing. Experiments are performed at 198.3-MHz ^{1}H frequency and 6.053-kHz (±5 Hz) MAS rate, with 668-μs double-quantum excitation (τ_{mix} = 1.3216 ms). In this case, a 5-mm rotor (Chemagnetics) is filled with ~120 mg of sample, providing an rf inhomogeneity of 6−8% fwhm. The decoupling field is incremented from 0 to >210 kHz in steps of approximately 2.2 kHz, and ^{13}C carrier frequency is approximately centered between the two signals. Signal due to natural abundance background is subtracted prior to calculation of DQF efficiency. The *y*-axis is normalized to the maximum observed CMR7 DQF efficiency (~70% of the total intensity observed in the CP-MAS experiment with π/2 pulses).

inhomogeneity (~±1−2%). In Figure 3a, the carrier is positioned on resonance (in the DQ subspace, where the sum of the two shifts is zero). The basic C7 sequence shows some sensitivity to error in the rf field amplitude, although the DQF efficiency is 40% or better over the range of 35−45 kHz. The optimal rf amplitude is slightly less than that predicted by theory (in part due to a ^{1}H decoupling effect discussed below), but in general the performance is acceptable for this two-spin system. Here, the CMR7 sequence offers improvement at higher rf field amplitude, a maximum of 62% DQF efficiency.

When the carrier is moved off-resonance by 5 kHz, the differences are even more pronounced. A severe sensitivity to the rf field amplitude is observed for the C7 sequence. Even when the nominal field amplitude is matched to the theoretical value (42 kHz), only 40% DQF efficiency is realized. In part, this is due to a distribution of rf fields over the sample. Also, crystallites with small effective dipolar couplings (due to the sin $2\beta_{PR}$ dependence) may be fully quenched by the chemical shift, resulting in little or no DQ coherence produced in those crystallites.

Finally, and perhaps of greatest significance, the heteronuclear decoupling dynamics exhibit strong dependence on mismatch of ^{1}H and ^{13}C rf field amplitudes.[29,63,64] This effect causes essentially irreversible loss of ^{13}C coherences into the ^{1}H bath, as illustrated in Figure 4. For the case of rotor-synchronized π pulses, mismatch of the rf field amplitudes by a factor of 3 greatly reduces the depolarization effect due to interference between the two rf fields. Although the theoretical approximation of π pulses is not directly applicable to windowless mixing sequences due to the time scale of ^{1}H−^{1}H interactions,[65] we find experimentally that the DQF filtration efficiency for CMR7 rapidly increases as a function of ^{1}H field until the factor of 3 is achieved (at ~125 kHz), at which point the rate of increase reduces substantially. This suggests that, in cases where decoupling fields are hardware-limited, substantial increases in DQF efficiency may be achieved by decreasing the MAS spinning rate (ω_r) or implementing sequences that require a lower multiple of ω_1:ω_r.[66]

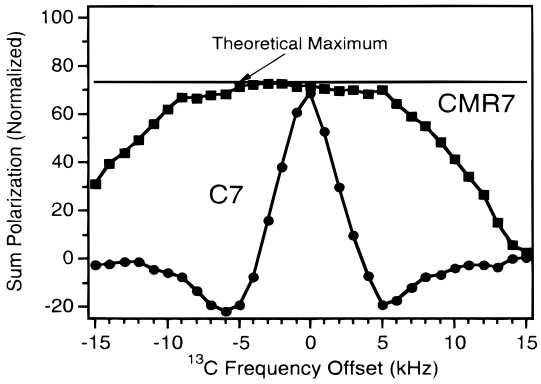

Figure 5. Bandwidth comparison for ^{13}C DQF of U-^{13}C,^{15}N-glycine (diluted to 10% with natural abundance material). The ^{1}H CW decoupling field during mixing is 160 kHz. Otherwise, experimental conditions are identical to those in Figure 4. The *y*-axis is normalized to the CP-MAS signal intensity (with π/2 pulses) at the corresponding frequency offset.

Referring back to Figure 3, with a ^{1}H decoupling field of 125 kHz, a more subtle demonstration of the ^{1}H−^{13}C interference effect is observed as an asymmetry in DQF efficiency as a function of ^{13}C rf field about the ideal theoretical value. In Figure 3a, the C7 DQF efficiency slopes downward at ^{13}C rf amplitudes higher than 35−45 kHz. Likewise, in Figure 3b, the CMR7 DQF efficiency is lower when the ^{13}C rf amplitude errs on the high side. Separate experiments (not shown here) indicate that lowering the decoupling field exacerbates this effect, and raising the decoupling field reduces the asymmetry. This result suggests another possible strategy for improved decoupling when ^{1}H field amplitudes are limited, namely reducing the ^{13}C field a few percent below the correct value; under these circumstances, the CMR7 compensation effectively removes the rf error and chemical shift terms, and the required ^{1}H field is reduced 3 times as rapidly as the ^{13}C field. Such an intentional reduction of rf field is particularly well tolerated for a two-spin system when the carrier is centered between the resonances, for the aforementioned reasons.

Figure 5 demonstrates broadband DQ excitation under the CMR7 sequence. With a ^{13}C rf field of 42 kHz, 50% or better DQF efficiency (3 dB below the theoretical maximum) is observed over a bandwidth of ±10.5 kHz; in contrast, the C7 sequence behaves selectively. Both sequences exhibit a slight frequency offset from zero chemical shift due to an asymmetric phase transient effect, which cancels a portion of the chemical shift due to rotation error. This effect is more pronounced in high Q probes and higher rf field strengths, and similar behavior has been observed in frequency-selective heteronuclear experiments.[45] Probe overcoupling[67] and/or optimization of the carrier frequency are essential only for C7, where slight differences from ideal conditions can lead to nontrivial DQF efficiency losses. However, the bandwidth of CMR7 implies that such empirical optimization is unnecessary.

Multispin Double-Quantum Filtration. Assuming that the two-spin DQ Hamiltonian is created over the CMR7 cycle with minimal dependence on chemical shift, additional spins can be considered within the approximation that each two-spin interaction is recoupled according to the zeroth-order theory. Multispin

(63) Ishii, Y.; Ashida, J.; Terao, T. *Chem. Phys. Lett.* **1995**, *246*, 439−445.

(64) Bennett, A. E. Ph.D. Thesis, Massachusetts Institute of Technology, 1995.

(65) Rienstra, C. M.; Bennett, A. E.; Sun, B.-Q.; Griffin, R. G. Manuscript in preparation.

(66) Hohwy, M. H.; Rienstra, C. M.; Jaroniec, C. P.; Griffin, R. G. Manuscript in preparation.

(67) Burum, D. P.; Linder, M.; Ernst, R. R. *J. Magn. Reson.* **1981**, *43*, 463−471.

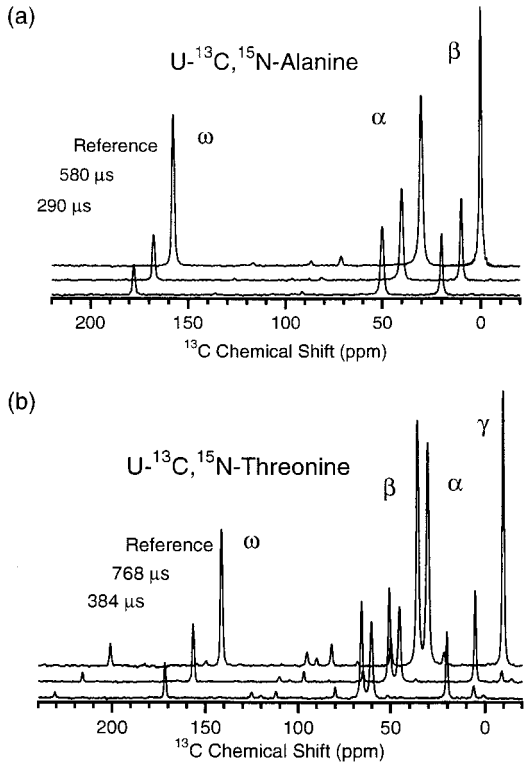

Figure 6. Experimental DQF spectra for multispin systems. In both cases, the rf carrier frequency is placed at approximately 100 ppm, and the DQ excitation time is annotated for comparison with the reference spectrum. The reference spectra are scaled to correct for natural abundance background signal. (a) U-^{13}C-Ala spectra were acquired at 317.4-MHz ^{1}H frequency, with 6.896-kHz (±5 Hz) MAS rate. CW ^{1}H decoupling (135 kHz) was used during the mixing period, and TPPM (100 kHz, 4.8 μs/15°) during acquisition. (b) U-^{13}C-Thr spectra were acquired at 397.8-MHz ^{1}H frequency, with 5.952-kHz (±5 Hz) MAS rate and 115-kHz CW ^{1}H decoupling during mixing. TPPM decoupling (80 kHz, 5.8 μs/15°) was used during the acquisition period. Short-time behavior can be approximated by the excitation and reconversion of DQ coherence between neighboring spin pairs. Longer filtering times result in more even distribution of polarization.

numerical simulations indicate that orientation-dependent effects in multispin chains may be observable.[48,68] However, in the present context, we are primarily concerned with the efficient excitation of DQ coherence for purpose of DQF experiments, with the intent of removing natural abundance background in cases where labeled clusters of spins are inserted within larger molecules.

Figure 6 demonstrates the three- and four-spin cases in the U-^{13}C-labeled amino acids Ala and Thr. At short times, polarization is shared almost equally between each spin in the DQ state. With 290-μs DQ excitation, the integrated intensities of ω-, α-, and β-^{13}C signals of Ala (normalized to the reference spectrum) are 22%, 43%, and 27%, respectively. The approximate 1:2:1 ratio is the result of equal distribution between spin pairs at short time, neglecting higher order coherences and weak couplings (e.g., ω to β). The significant CSA of the ω-^{13}C signal causes a slight reduction of intensity relative to the β. However, this asymmetry is reduced upon longer mixing, due to the additional compensation for higher order CSA effects provided by the CMR7 supercycle. At 580-μs DQ excitation, the intensities of 30%, 57%, and 34% correspond to higher total efficiency, and the 1:2:1 ratio is still approximately correct.

In the four-spin system of U-^{13}C-Thr, the corresponding behavior is observed at short mixing time. With 384-μs DQ excitation, the relative integrated intensities (from left to right in the spectra shown) for ω, β, α, and γ are 25%, 42%, 37%, and 23%, respectively. Here the intensity ratio of 1:2:2:1 is approximately correct. At longer mixing time (768-μs DQ excitation), the outer spins increase in intensity (ω to 43%, γ to 33%), while the inner spins remain almost constant (β at 41%, α at 37%). We have explored this behavior in larger spin systems as well, where the effects are qualitatively similar. Experiments with larger U-^{13}C-labeled amino acids and peptides suggest that it is possible to achieve DQF efficiencies of at least 40−45% for spins within a continuous chain and slightly less for spins at or near the end of chains. In general, the optimal total mixing time for DQF in multispin ^{13}C systems is slightly less (~0.8−1.0 ms total excitation and reconversion time) than that in the two-spin case (1.3 ms). At longer mixing times (1.2−1.5 ms), the total polarization is distributed to the ends of the chain more evenly, although the total integrated intensity decreases rapidly. This signal loss may be due to the creation of higher order (2*n*-quantum) coherences, which show greater sensitivity to experimental imperfections such as phase transients, calibration errors, and amplitude imbalances among nonorthogonal transmitter phases. Because total coherence order is not conserved, in contrast to the analogous ZQ experiments,[69] not all polarization is reconverted to observable coherence for detection, and cancellation may occur during reconversion of DQ coherences in a multispin environment. These considerations suggest that, in the present context, shorter mixing times are most appropriate for DQF experiments in multispin systems.

Two-Dimensional $^{13}C-^{13}C$ Chemical Shift Correlation Spectroscopy. Several sequences, including RFDR,[28,29] MELODRAMA,[34,49] DRAWS,[35−37] and RIL,[70,71] have been applied to $^{13}C-^{13}C$ chemical shift correlation spectroscopy. Although the latter three sequences also offer dipolar recoupling which is insensitive to chemical shift and tolerant of rf errors, the CMR7 DQ mixing scheme does so with significant improvement in theoretical cross-peak intensity. With 73% polarization transfer, the ratio of cross-peak to diagonal intensity would be expected to be almost 3:1, and in two-spin cases such as U-^{13}C,^{15}N-Gly, we have observed better than 2:1 relative intensities in 2D spectra (not shown). However, as demonstrated in the three- and four-spin DQF experiments above, the full theoretical DQF efficiency is not realized in multispin systems, and similar behavior is observed in correlation spectra with respect to cross-peak intensities. Nevertheless, in many cases, cross-peak intensities exceed the diagonal peaks, and in favorable instances the ratio of intensities is greater than 2:1, even in the multispin limit.

Although 2D correlation spectra can be implemented with DQF,[68] there are several advantages to constant DQ phase mixing. In either implementation, cross-peaks arise only from pairs of ^{13}C spins. However, with the filter, half of the selected DQ coherence is reconverted to the diagonal peak (in the two-spin case). For many applications, this diagonal peak intensity provides little additional information and may obscure cross-peaks near the diagonal, in particular when cross-peaks have the same sign (as is the case for the standard DQF 2D implementation). In addition, we have observed that multiple-bond cross-peaks appear with greater relative intensity without

(68) Geen, H.; Gottwald, J.; Graf, R.; Schnell, I.; Spiess, H. W.; Titman, J. T. *J. Magn. Reson.* **1997**, *125*, 224−227.

(69) Bruschweiler, R.; Ernst, R. R. *J. Magn. Reson.* **1997**, *124*, 122−126.

(70) Baldus, M.; Tomaselli, M.; Meier, B. H.; Ernst, R. R. *Chem. Phys. Lett.* **1994**, *230*, 329−336.

(71) Baldus, M.; Meier, B. H. *J. Magn. Reson.* **1997**, *128*, 172−193.

Table 2. Chemical Shifts for U-^{13}C-Erythromycin A Assigned via the 2D CMR7 ^{13}C−^{13}C Correlation Spectrum[a]

position	chemical shift (ppm)	position	chemical shift (ppm)
9	221.0	1	176.1
1	176.1	2	44.8
1′	102.7	3	79.4
1″	95.8	4	39.2
5	83.1	5	83.1
3	79.4	6	73.8
4″	78.5	7	38.7
13	76.7	8	45.3
12	74.3	9	221.0
6	73.8	10	37.2
3″	72.4	11	68.4
2′	71.1	12	74.3
11	68.4	13	76.7
5′	68.2	14	21.6
3′	65.5	15	10.6
5″	65.3	16	15.7
8″	49.2	17	9.6
8	45.3	18	26.2
2	44.8	19	17.9
4	39.2	20	12.1
7	38.7	21	16.5
10	37.2	1′	102.7
2″	35.7	2′	71.1
4′	28.9	3′	65.5
18	26.2	4′	28.9
14	21.6	5′	68.2
7″	21.6	6′	21.3
6′	21.3	1″	95.8
6″	18.9	2″	35.7
19	17.9	3″	72.4
21	16.5	4″	78.5
16	15.7	5″	65.3
20	12.1	6″	18.9
15	10.6	7″	21.6
17	9.6	8″	49.2

[a] Peaks are referenced to the 2-^{13}C resonance of glycine at 43.5 ppm. Digital resolution is 0.25 ppm. (The 7′ and 8′ signals are not observed in the correlation spectrum, due to motional averaging of the dimethylamino group at room temperature.[81,82])

the DQ filter. Filtration does, of course, scale the natural abundance background signal and, therefore, may be of use for applications to spin labels within larger molecules, despite the fact that sensitivity in the information-rich cross-peak region is reduced. Yet, for smaller molecules, the constant phase DQ mixing provides superior spectra in our experience.

An illustrative example of these effects and the improvement in resolution observed upon extending to a second ^{13}C chemical shift dimension is provided by the 2D correlation spectrum of U-^{13}C-labeled erythromycin A (Figure 7). Erythromycin A is a macrolide antibiotic that inhibits protein synthesis by binding to bacterial ribosomes. A number of structural studies have been performed on this molecule using solution-state NMR[72−77] and X-ray crystallography.[78,81] The erythromycin−ribosome complex exhibits a solid-state NMR spectrum even in solution and motivates the solid-state studies of free erythromycin A.

The spectrum shown in Figure 7b allows the unambiguous assignment of all resonances which have directly bonded ^{13}C neighbors and represents an important first step for future structural studies. Of particular utility are the regions of cross-peaks near the diagonal (65−85 ppm), corresponding to the hexose rings where chemical shift dispersion is minimal. The resolution in this region is significantly better than that observed with ZQ mixing methods, such as RFDR and ^{1}H-driven spin diffusion[79] (data not shown). In part, this is due to improved polarization transfer efficiency between spins of small chemical shift difference. However, an additional important consideration is the improved contrast and dynamic range implied by the DQ transfer. A minority of the total polarization remains on the diagonal, and so this uninformative part of the spectrum is deemphasized; also because the diagonal and cross-peak differ in sign, a sharp delineation is observed between the two. Cancellation of cross-peaks due to degeneracies of opposite sign are not significant in this spectrum, although partial cancellation can lead to slight distortions of the line shape and uncertainties in chemical shift (in the absence of explicit line shape simulations). Note that, in one case (C-3′ to C-5′), a two-bond DQ transfer of resonances of small chemical shift difference provides a line shape similar to that observed under ZQ transfer. This is manifested as a broadening of the diagonal that is often experimentally indistinguishable from the line shape asymmetries that arise due to uneven initial polarization and nonideal ^{1}H decoupling conditions.[80]

An additional advantage of the DQ mixing scheme lies in the identification of two-bond cross-peaks (e.g., from C-1′ to C-3′ and C-1″ to C-3″); these peaks are valuable for confirming the assignment in the congested hexose region and are unambiguously distinguished from one-bond transfers due to the sign difference. Significant polarization transfer through weaker couplings (e.g., the 500-Hz two-bond couplings of C-3 to C-1″, C-5 to C-1′, C-3′ to C-7′ and C-8′, etc.) is not observed when multistep transfer pathways through strong (∼2−2.2 kHz) couplings exist.[43,46,47] However, in one case, where a strong-coupling pathway is not available, direct transfer through a 500-Hz coupling is observed (C-3″ to C-8″). The intensity of this cross-peak is substantially weaker than many of those that arise due to two-step transfers (e.g., C-1′ to C-3′, C-1″ to C-3″, C-3 to C-16, C-5 to C-17, etc.), but the direct transfer is unambiguous due to the sign of the cross-peak. Only the C-7′ and C-8′ resonances are not assigned from the 2D spectrum, due to motional averaging of the C-3′ to C-7′ and C-3′ to C-8′ couplings.[81,82]

Conclusions

We have demonstrated that the theoretical advantages of the C7 sequence of Lee et al.[1] may be applied in a more experimentally robust manner. By refocusing the dominant error terms due to chemical shifts and rf errors, a DQ dipolar Hamiltonian can be created under MAS conditions with high efficiency over a bandwidth of approximately ±10 kHz. This allows for potential applications of CMR7 up to ^{1}H frequencies of at least 400 MHz in multispin systems experiencing a large range of chemical shifts, both isotropic and anistropic. The ability to excite and filter DQ coherence with high

(72) Barber, J.; Gyi, J. I.; Morris, G. A.; Pye, D. A.; Sutherland, J. K. *J. Chem. Soc., Chem. Commun.* **1990**, *15*, 1040−1041.
(73) Barber, J.; Gyi, J. I.; Lian, L.; Morris, G. A.; Pye, D. A.; Sutherland, J. K. *J. Chem. Soc., Perkin Trans. 2* **1991**, *10*, 1489−1494.
(74) Barber, J.; Gyi, J. I.; Pye, D. A. *J. Chem. Soc., Chem. Commun.* **1991**, *18*, 1249−1252.
(75) Cane, D. E.; Hasler, H.; Taylor, P. B.; Liang, T.-C. *Tetrahedron* **1983**, *39*, 3449−3455.
(76) Pye, D. A.; Gyi, J. I.; Barber, J. *J. Chem. Soc., Chem. Commun.* **1990**, *17*, 1143−1145.
(77) Everett, J. R.; Tyler, J. W. *J. Chem. Soc., Perkin Trans. 2* **1987**, 1659−1667.
(78) Perun, T. J.; Egan, R. S. *Tetrahedron Lett.* **1969**, *5*, 387−390.
(79) Kubo, A.; McDowell, C. A. *J. Chem. Soc., Faraday Trans. 1* **1988**, *84*, 3713−3730.
(80) Sun, B. Q.; Rienstra, C. M.; Costa, P. R.; Williamson, J. R.; Griffin, R. G. *J. Am. Chem. Soc.* **1997**, *119*, 8540−8546.
(81) Stephenson, G. A.; Stowell, J. G.; Toma, P. H.; Pfeiffer, R. R.; Byrn, S. R. *J. Pharm. Sci.* **1997**, *86*, 1239−1244.
(82) McGeorge, G. Private communication, 1998.

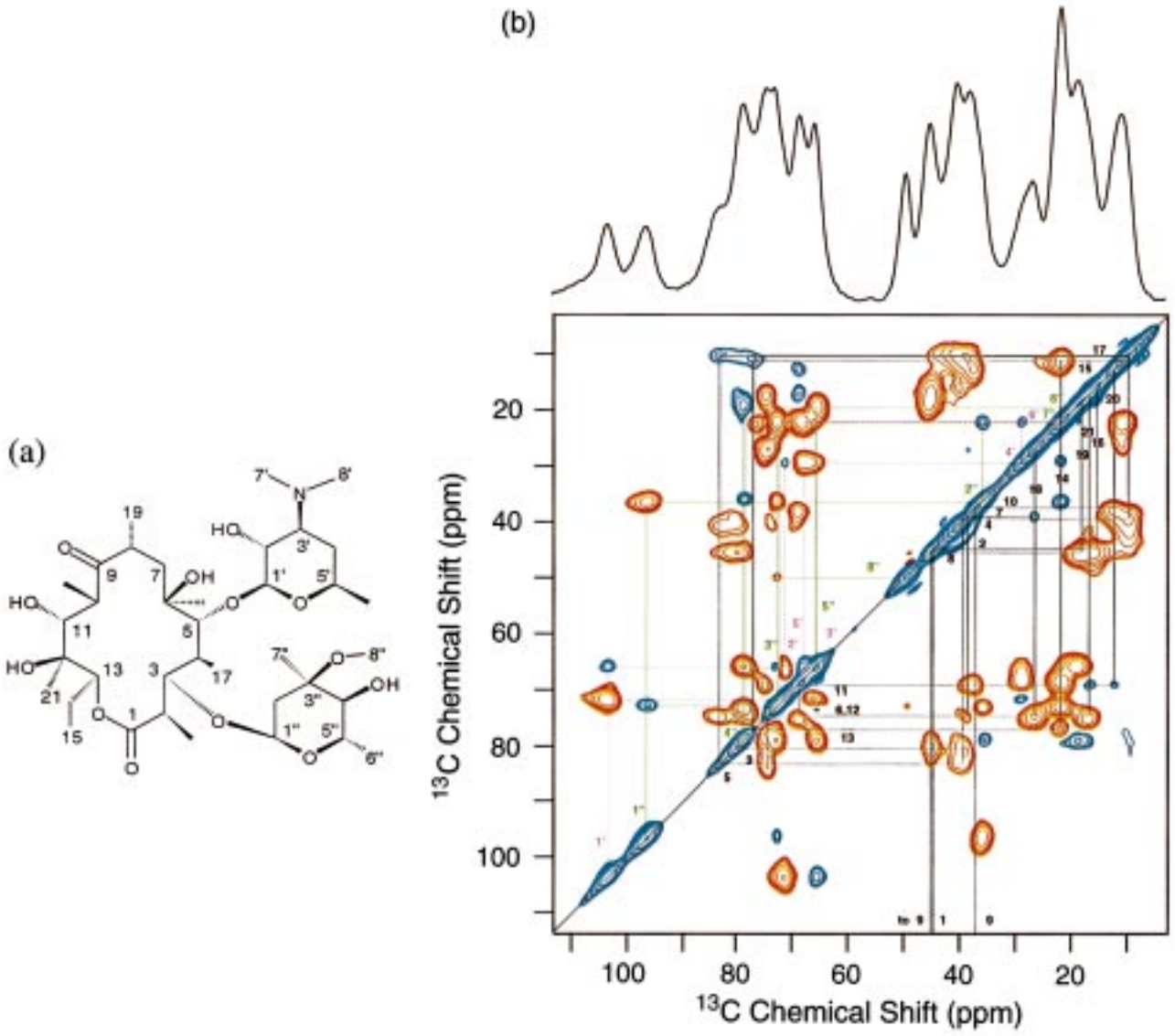

Figure 7. (a) Chemical structure and (b) 2D $^{13}C-^{13}C$ chemical shift correlation spectrum of U-^{13}C-erythromycin A, which consists of a 14-member lactone ring with desosamine (labeled prime) and cladinose (labeled double prime) sugar substituents. Experimental conditions for DQ mixing are the same as in Figure 3, with the following exceptions: (1) MAS rate is 8.00 kHz (±5 Hz); (2) mixing time is 1.0 ms; and (3) rotor volume is fully utilized with ~30−35 mg of sample; and (4) the phase of the DQ Hamiltonian is constant throughout the mixing period. Two-dimensional data processing includes sine bell and exponential apodization functions in each dimension. Ten contour levels are logarithmically spaced over the range of 1%−100% of maximum peak amplitude (positive in blue, negative in red). The diagonal peaks are numbered and cross-peaks labeled with a color-coded scheme as follows: black for the macrocyclic ring, magenta for the desosamine, and green for the cladinose.

efficiency in such multispin systems facilitates the use of U-^{13}C-labeled molecules within a large natural abundance background. In addition, correlation spectroscopy of similar systems permits more expedient and cost-effective determination of chemical shifts and allows the unambiguous assignment of spin labels.

The 2D $^{13}C-^{13}C$ correlation spectrum of erythromycin A provides a vivid example of the enhanced resolution by extension to a second chemical shift dimension. Although other DQ[34,35,37,49,80] and/or ZQ[28,29,70,71,83] recoupling methods may also produce correlation spectra of high quality, the improved cross-peak intensities observed with the CMR7 method are a significant advantage in larger spin systems, where sensitivity is problematic. In addition, the alternation of cross-peak intensities from negative to positive, etc. (characteristic of DQ mixing), is a valuable tool in the assignment process in cases such as erythromycin A, where multiple degeneracies exist in the 1D ^{13}C spectrum and one-bond correlations alone are not sufficient to make unambiguous assignments.

Beyond the assignment and filtering applications, extensions of dipole−dipole correlation experiments are possible with the CMR7 sequence. By incorporating a third dimension of heteronuclear dipolar evolution (e.g., $^{1}H-^{13}C$ or $^{13}C-^{15}N$) into the chemical shift correlation experiment, each correlated pair in the 2D $^{13}C-^{13}C$ spectrum may be constrained with respect to the relative orientation of the attached ^{1}H or ^{15}N spins. Such an experiment could constrain several $^{1}H-^{13}C-^{13}C-^{1}H$[7,8] or $^{15}N-^{13}C-^{13}C-^{15}N$[9,12] torsion angles in a single experiment.

Finally, we note that the compensation scheme presented here is generally applicable and does not perturb the symmetry inherent to C*n* sequences, where each unit has time-reflection symmetry and the overall sequence is organized according to

(83) Boender, G. J.; Raap, J.; Prytulla, S.; Oschkinat, H.; de Groot, H. J. M. *Chem. Phys. Lett.* **1995**, *237*, 502−508.

the coherence order desired. (This, in general, is not true in sequences that superimpose π or $\pi/2$ pulses over the basic unit.) Therefore, we anticipate that similar compensation schemes will facilitate applications with other types of windowless mixing sequences.

Acknowledgment. The authors thank M. Jackson, D. Zeidner, and R. Summers for the preparation of U-^{13}C-erythromycin A and acknowledge NIH support of this research via grants RR-00995, GM-36810, GM-23403, and GM-23289 and a postdoctoral fellowship for M.E.H. L.J.M. is an American Cancer Society Postdoctoral Fellow, and C.M.R. is a Howard Hughes Medical Institute Predoctoral Fellow. Insightful discussions with John D. Gross and Dr. Marc A. Baldus are appreciated, as are the critical reading of the manuscript by Prof. Judith Herzfeld (Brandeis University) and the technical expertise of Dr. David J. Ruben.

JA9810181